J Bioenerg Biomembr (2008) 40:587–598
DOI 10.1007/s10863-008-9184-4

Mitochondrial generation of reactive oxygen species is enhanced at the Q_o site of the complex III in the myocardium of *Trypanosoma cruzi*-infected mice: beneficial effects of an antioxidant

Jian-Jun Wen · Nisha Jain Garg

Received: 18 September 2008 / Accepted: 3 October 2008 / Published online: 14 November 2008
© Springer Science + Business Media, LLC 2008

Abstract In this study, we have characterized the cellular source and mechanism for the enhanced generation of reactive oxygen species (ROS) in the myocardium during *Trypanosoma cruzi* infection. Cardiac mitochondria of infected mice, as compared to normal controls, exhibited 63.3% and 30.8% increase in ROS-specific fluorescence of dihydroethidium (detects $O_2^{\bullet-}$) and amplex red (detects H_2O_2), respectively. This increase in ROS level in cardiac mitochondria of infected mice was associated with a 59% and 114% increase in the rate of glutamate/malate- (complex I substrates) and succinate- (complex II substrate) supported ROS release, respectively, and up to a 74.9% increase in the rate of electron leakage from the respiratory chain when compared to normal controls. Inhibition studies with normal cardiac mitochondria showed that rotenone induced ROS generation at the Q_{Nf}-ubisemiquinone site in complex I. In complex III, myxothiazol induced ROS generation from a site located at the Q_o center that was different from the Q_i center of $O_2^{\bullet-}$ generation by antimycin. In cardiac mitochondria of infected mice, the rate of electron leakage at complex I during forward (complex I-to-complex III) and reverse (complex II-to-complex I) electron flow was not enhanced, and complex I was not the main site of increased ROS production in infected myocardium. Instead, defects of complex III proximal to the Q_o site resulted in enhanced electron leakage and ROS formation in cardiac mitochondria of infected mice. Treatment of infected mice with phenyl-α-tert-butyl-nitrone (PBN) improved the respiratory chain function, and, subsequently, decreased the extent of electron leakage and ROS release. In conclusion, we show that impairment of the Q_o site of complex III resulted in increased electron leakage and $O_2^{\bullet-}$ formation in infected myocardium, and was controlled by PBN.

Keywords Chagas disease · Mitochondria · Myocardium · Reactive oxygen species · Electron transport chain · Site of ROS production

Abbreviations

Amplex red	10-acetyl-3, 7-dihydroxyphenoxazine
CAT	catalase
Complex I	NADH ubiquinone oxidoreductase
Complex III	ubiquinol cytochrome c oxidoreductase
Complex IV	cytochrome c oxidase
Complex V	F_1F_o ATP synthase
Cyt b_L and Cyt b_H	cytochrome b low- and high-potential hemes, respectively
DHE	dihydroethidium
FAD	flavin adenine dinucleotide
FMN	flavin mononucleotide

J.-J. Wen · N. J. Garg
Departments of Microbiology and Immunology,
University of Texas Medical Branch,
301 University Blvd,
Galveston, TX 77555-1070, USA

N. J. Garg
Department of Pathology, University of Texas Medical Branch,
Galveston, TX, USA

N. J. Garg
Member of the Institute for Human Infections
and Immunity and Sealy Center for Vaccine Development,
University of Texas Medical Branch,
Galveston, TX, USA

N. J. Garg (✉)
3.142C Medical Research Building,
University of Texas Medical Branch,
301 University Boulevard,
Galveston, TX 77555-1070, USA
e-mail: nigarg@utmb.edu

Glu/Mal	glutamate/malate
HRP	horseradish peroxidase
ISP	Rieske [Fe-S] protein
PBN	phenyl-α-tert-butyl nitrone
Q/QH_2	oxidized/reduced (hydroquinone, quinol) form of quinone
Q_i/Q_o	quinine-reducing/quinol-oxidizing sites of complex III
SOD	superoxide dismutase
Succ	succinate
T. cruzi	*Trypanosoma cruzi*

Introduction

Chagas disease is a major human health problem in the southern parts of the American continent (WHO 2002). Preclinical and clinical studies have shown that hosts infected by *Trypanosoma cruzi* are presented with oxidative overload (Zacks et al. 2005). The cytotoxicity of reactive oxygen species (ROS) is related to their ability to oxidize cell constituents that leads to a deterioration of the cellular structure and function, and, ultimately, to cell death. We have demonstrated a decline in antioxidant capacity and an increase in lipid and protein oxidation in the myocardium of infected mice with progressive disease (Wen et al. 2004). Increased plasma level of malonyldialdehydes (MDA) and glutathione disulfide (GSSG), associated with decreased levels of glutathione defense and superoxide dismutase (SOD), is shown in chagasic patients (Wen et al. 2006b), suggesting that an antioxidant/oxidant imbalance ensues during Chagas disease.

Electron microscopic analysis of the myocardial biopsies from chagasic patients and experimental animals has identified that the mitochondrial degenerative changes occur during disease progression (Carrasco Guerra et al. 1987; Palacios-Pru et al. 1989; Garg et al. 2003; Wen et al. 2006b). Other studies showed that alterations in the expression of mitochondrial DNA-encoded genes contributed to respiratory inefficiency and impaired ATP formation in *T. cruzi*-infected murine hearts (Vyatkina et al. 2004). Treatment of infected mice with an antioxidant partially restored the respiratory complex activities (Wen et al. 2006a), thus, indicating a role of oxidative overload in the corroboration of mitochondrial defects in chagasic hearts.

A low, but constant, production of superoxide ($O_2^{\bullet-}$) occurs in mitochondria because of the electron leakage from the respiratory chain to O_2 (Boveris et al. 1972). The rate of electron leakage and $O_2^{\bullet-}$ formation in mitochondria is closely related to the coupling efficiency between the respiratory chain and oxidative phosphorylation (Boveris et al. 1972). Our observations of a decline in the complex I and complex III activities in chagasic hearts (Vyatkina et al. 2004) suggested that the efficient transfer of electrons across the respiratory chain to complex IV may not be maintained. If such is the case, an increased leakage of electrons to O_2 within the respiratory chain may result in increased mitochondrial ROS toxicity in infected myocardium. Accordingly, the purpose of this study was to determine whether mitochondrial ROS production is increased in the myocardium of *T. cruzi*-infected mice, and if so, to identify the site of ROS formation in the electron transport chain. The assembly of complex I and complex III, and their efficiency to transfer electron energy for ATP formation are susceptible to oxidative stress (Wen et al. 2006a). We, therefore, chose to treat the infected mice with phenyl-α-tert-butyl-nitrone (PBN) antioxidant, shown to protect mitochondria from oxidative injuries (Floyd et al. 2002). We envisaged that enhancing the antioxidant capacity would arrest the oxidative damage-induced inefficient electron transfer through the respiratory chain, and thereby, reduce mitochondrial ROS generation. Our findings show that enhanced production of $O_2^{\bullet-}$ in cardiac mitochondria of *T. cruzi*-infected mice occurs due to a functional block at a site within complex III. PBN treatment effectively decreased the rate of ROS generation through preservation of complex III functional activity and respiratory chain efficiency in infected mice.

Experimental procedures

Mice and parasites Six-to-8-week-old male C3H/HeN mice (Harlan) were infected with *T. cruzi* trypomastigotes (SylvioX10/4 strain, 10,000/mouse), and treated with PBN (50 mg/kg, twice a week, i.p.). Mice were sacrificed in acute infection phase (27–35 days post-infection). Animal experiments were performed according to the National Institutes of Health Guide for Care and Use of Experimental Animals and approved by the UTMB Animal Care and Use Committee.

Isolation of mitochondria Freshly harvested tissues or tissues frozen at −80°C were minced in ice-cold HMSB medium (10 mM HEPES pH 7.4, 225 mM mannitol, 75 mM sucrose, and 0.2% fatty acid free BSA, tissue: buffer ratio, 1:20) and homogenized in a dounce homogenizer in presence of 20 U/ml collagenase. Collagenolysis was stopped with addition of 1 mM EGTA, and mitochondria were isolated by differential centrifugation (Toth et al. 1986). All mitochondrial preparations consisted <5% of peroxisome and endoplasmic reticulum contamination, determined by measurement of acid phosphatase (Lui et al. 1968) and glucose-6-phosphatase (Harper 1963) activities, respectively. Protein content was measured by the Bradford method (Bradford 1976).

ROS level Mitochondria (25-μg protein) were suspended in 10 mM Tris-HCl at pH 7.4, 250 mM sucrose, 1 mM EDTA, and added in triplicate to 96-well, black flat-bottomed plates. Mitochondria were incubated with 30 μM dihydroethidium (DHE) for 30 min, and ROS-mediated formation of fluorescent ethidium was recorded at Ex_{498nm}/Em_{598nm}, using a SpectraMax M2 microplate reader (Molecular Devices). To confirm ROS level, mitochondria were incubated for 30 min with 33 μM 10-acetyl-3, 7-dihydroxyphenoxazine (amplex red, Invitrogen) and 0.1 U/ml horseradish peroxidase (HRP). The HRP-catalyzed, ROS-mediated amplex red oxidation, resulting in fluorescent resorufin formation, was monitored at Ex_{563nm}/Em_{587nm}. To determine the specificity of DHE and amplex red for $O_2^{\bullet-}$ and H_2O_2, respectively, reactions were performed in presence of 1 μM CuZnSOD (removes $O_2^{\bullet-}$) or 0.3 μM catalase (CAT, removes H_2O_2). Standard curves were prepared with ethidium (0–15 μM) and H_2O_2 (50 nM–5 μM).

Rate and site of ROS production Mitochondria (25-μg protein) were energized with complex I (10 mM glutamate/ 5 mM malate (glu/mal)) or complex II (5 mM succinate (succ)) substrates. The rate of ROS generation was monitored using amplex red/HRP or DHE fluorescent probes with an online addition of specific inhibitors of respiratory complexes. Complex I inhibitors: 6.35 μM rotenone (Rot, binds to Q_{Nf} and Q_{Ns} sites), 2 mM p-chloromercuribenzoate (pCMB, binds to $[Fe\text{-}S]_{N1b}$ cluster), and 10 μM diphenylene iodonium (DPI, binds to $[Fe\text{-}S]_{N1a}$). Complex II inhibitors: 1 mM 3-nitropropionic acid (3-NPA, binds to succinate dehydrogenase) and 2.5 mM malonate (*binds* to the active site of the succinate dehydrogenase). Complex III inhibitors: 3.75 μM antimycin (Ant, binds to Q_i site of Q cycle near cyt b_H), 10 μM myxothiazol (Myx, binds to Q_o site of Q cycle near cyt b_L), and 10 μM stigmatellin (Stig, binds to Q_o site near the Reiske protein).

Rate of electron leakage Mitochondria were utilized under similar assay conditions to measure $O_2^{\bullet-}$ production using DHE, and O_2 consumption using a Mitocell S200A Respirometry System (Strathkelvin, Motherwell, UK), as described (Sanz et al. 2005). Briefly, for respiration, mitochondria (200-μg) were suspended in a mitocell containing 0.5 ml MSP medium (225 mM mannitol, 75 mM sucrose, 20 mM KH_2PO_4/K_2HPO_4 pH 7.6), and substrate-stimulated O_2 consumption was recorded. The percentage of electron leakage was calculated as the rate of $O_2^{\bullet-}$ production X 100/2 X rate of O_2 consumption. The concentration of O atoms in air-saturated medium was assumed to be 276 μM (Lemasters 1984).

Enzyme assays The oxidation of NADH by complex I was recorded using 2, 3-dimethoxy-5-methyl-6-decyl-1, 4-benzoquinone (DB) as an electron acceptor (ε=6.1 $mM^{-1}.cm^{-1}$). The oxidation of DBH_2 by complex III was determined using cytochrome c as an electron acceptor (ε=19.1 $mM^{-1}.cm^{-1}$). Specific activities were evaluated after subtracting the background absorbance (<10%) obtained in the presence of specific inhibitors (Jarreta et al. 2000; Vyatkina et al. 2004).

Data analysis Data are expressed as means±SD, and were derived from at least triplicate observations per sample (n ≥ nine animals/group). Results were analyzed for significant differences using ANOVA procedures and Student's t-tests. The level of significance was accepted at $P<0.01$ (* infected versus normal controls, # infected/PBN-treated versus infected/untreated).

Results

The basal ROS level in isolated cardiac mitochondria was monitored using DHE (Fig. 1a) and amplex red probes (Fig. 1b). Cardiac mitochondria from infected mice showed a 63% increase in DHE oxidation (detected by formation of fluorescent ethidium, Fig. 1a) and 31% increase in amplex red oxidation (detected by formation of fluorescent resorufin, Fig. 1b) as compared to that detected in normal controls. These results demonstrated that mitochondrial ROS level was elevated in the myocardium of infected mice.

Before we examined the rate and site of increased ROS release in cardiac mitochondria of infected mice, it was important to determine the specificity of the probes and validate whether frozen mitochondria can be used for measuring the rate of ROS release. DHE oxidation and formation of fluorescent ethidium was decreased by 53% (range 33%–53%) when mitochondria were incubated with CuZnSOD (converts $O_2^{\bullet-}$ to H_2O_2, Fig 1a), suggesting that $O_2^{\bullet-}$ is not highly diffusible across mitochondrial membranes. The specificity of amplex red for H_2O_2 was confirmed by ~80% decline in fluorescence when mitochondrial preparations were incubated with catalase (converts H_2O_2 to water, Fig. 1b). No effect of CuZnSOD was observed on amplex red oxidation. Background fluorescence obtained with a reaction mixture without mitochondria was almost negligible. None of the inhibitors of respiratory complexes that we intended to use in this study showed a non-specific oxidation of amplex red in absence of mitochondria. These data validated the specificity and sensitivity of amplex red for monitoring ROS (H_2O_2) production.

Next, we isolated mitochondria from freshly collected and frozen heart tissues and monitored the rate of ROS

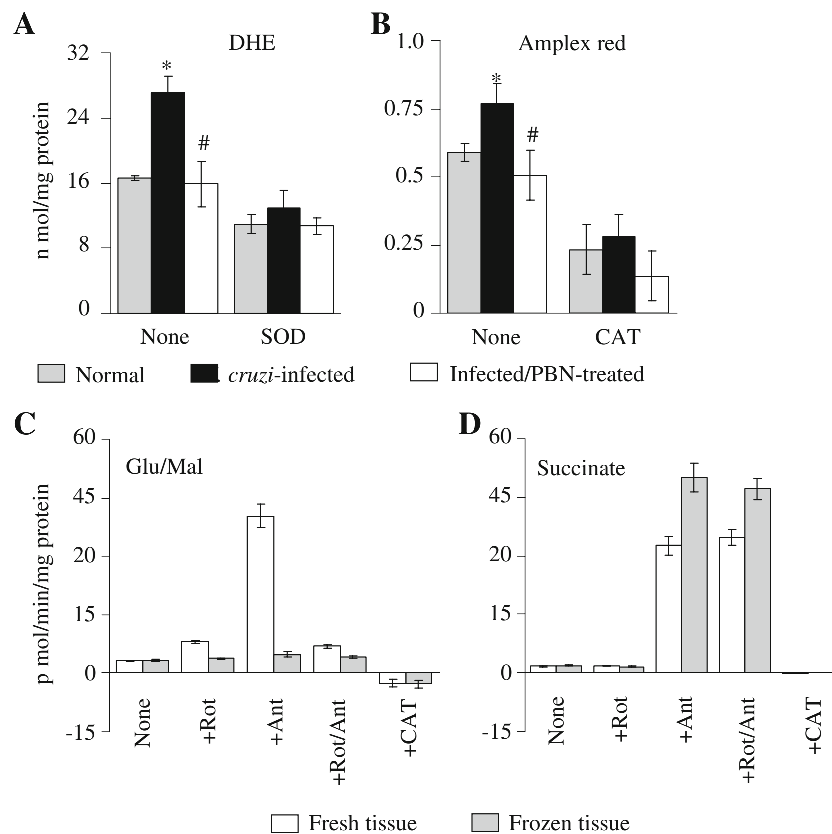

Fig. 1 **a & b** ROS levels in cardiac mitochondria of *T. cruzi*-infected mice (±PBN). C3H/HeN mice were infected with *T. cruzi* and treated with PBN. Mice were sacrificed during acute phase and cardiac mitochondria isolated by differential centrifugation were incubated with ROS-sensitive DHE (**a**) or amplex red (**b**) fluorescent probes. The effect of superoxide dismutase (SOD) and catalase (CAT) on ROS levels was monitored to validate the specificity of fluorescent probes. (C & D) Rate of ROS production in mitochondria isolated from fresh and frozen tissues. Cardiac mitochondria, isolated from freshly harvested or frozen heart tissue of normal mice, were incubated with glutamate/malate (**c**) or succinate (**d**) substrates, and the rate of amplex red oxidation was monitored in the presence of rotenone (Rot), antimycin (Ant) or CAT. Data (mean±SD) are representative of three independent experiments (n=9/group). $^{*,\#}p<0.01$ (* infected versus normal, $^{\#}$ infected/PBN-treated versus infected/untreated)

production. Cardiac mitochondria isolated from freshly collected tissues, fed with glu/mal (complex I substrates), responded to rotenone or antimycin (individually or together) addition by an increase in amplex red oxidation (Fig. 1c). Mitochondria isolated from frozen tissues did not exhibit glu/mal-dependent, rotenone- and/or antimycin-induced increase in ROS formation (Fig. 1c). Cardiac mitochondrial preparations from both fresh and frozen tissues, fed with succinate (complex II substrate), exhibited rotenone-independent, antimycin-induced increase in amplex red oxidation (Fig. 1d). These data suggest that cardiac mitochondria from frozen tissues can be utilized to examine ROS production from a site upstream of complex II; however, it is necessary to use fresh mitochondria for monitoring the complex I-dependent ROS release.

Based upon the above experiments, we chose amplex red probe to evaluate the rate and site of ROS release in cardiac mitochondria isolated from freshly harvested tissues from infected mice. Cardiac mitochondria from infected mice energized with glu/mal or succinate substrates exhibited 59% and 114% higher rate of amplex red-dependent H_2O_2 generation, respectively, as compared to that noted in normal controls (Fig. 2a, Tables 1, 2). Previously, we have documented that the activities of the complex I and complex III were decreased in cardiac mitochondria of infected mice by 39% and 59%, respectively (complex I: 121.74±13.7 versus 198.37±30.24 n mol/mg protein/min, complex III: 175.57±16.5 versus 424.09±47.15 n mol/mg protein/min, infected versus normal) (Wen et al. 2006a). To determine if decreased activities of the respiratory complexes result in increased electron leakage to molecular O_2 and ROS generation, we monitored the rate of O_2 consumption and electron leakage. Cardiac mitochondria from normal and infected mice exhibited a similar rate of oxygen consumption per min when energized with glu/mal or succinate substrates (data not shown). Despite no change in respiration, infected cardiac mitochondria exhibited a 74% and 173% increase in the rate of electron leakage

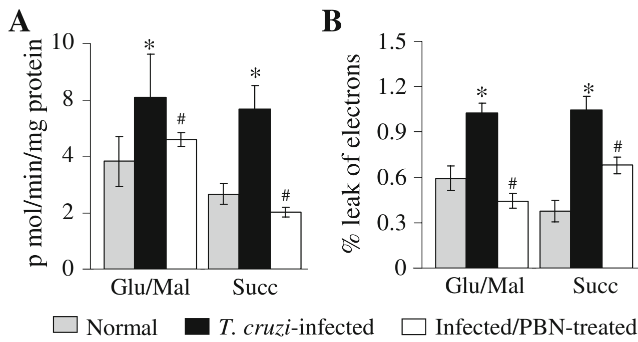

Fig. 2 Rate of cardiac mitochondrial ROS generation and electron leakage in infected mice (±PBN). Freshly isolated cardiac mitochondria from normal, infected, and infected/PBN-treated mice were energized with complex I (glu/mal) or complex II (succinate) substrates. The rates of H_2O_2-dependent amplex red oxidation (**a**) and electron leakage (**b**) were monitored as described in Materials and Methods. Data (mean±SD) are representative of three independent experiments (n=9/group, $^{*,\#}p<0.01$)

when energized with glu/mal and succinate substrates, respectively (Fig. 2b). Together, these results show that enhanced electron leakage from the respiratory chain result in increased ROS formation in cardiac mitochondria of infected mice.

In PBN-treated/infected mice, the cardiac mitochondrial level of ROS (Figs. 1a,b) and the rate of glu/mal- and succinate-supported ROS generation (Fig. 2a) were normalized to the control levels. This decline in mitochondrial ROS generation in PBN-treated/infected mice was associated with a 100% control of glu/mal-dependent electron leakage and 35% decline in succinate-dependent electron leakage when compared to the untreated/infected mice (Fig. 2b). We also noted the myocardial respiratory complex activities was significantly improved in PBN-treated/infected mice (Complex I: 192.8±26.7 versus 121.7±13.7 nmol/min/mg protein, Complex III: 316.2±28.8 versus 175.6±16.5 n mol/min/mg protein, infected/PBN-treated versus infected/untreated, $p<0.001$). These results showed that PBN treatment of infected mice preserved the electron transport chain activity, and thereby, resulted in decreased electron leakage and mitochondrial ROS formation in infected myocardium. No statistically significant changes were observed in the rate of mitochondrial ROS generation and electron leakage when normal mice were treated with PBN (data not shown).

We proceeded to investigate *a*) what are the possible site (s) of electron leakage and ROS formation in murine mitochondria, and, *b*) which of these sites is defective resulting in increased ROS production in infected myocardium. For this, we treated isolated cardiac mitochondria with metabolic inhibitors of respiratory complexes, and monitored the rate of ROS release. We anticipated that inhibitors would provide an altered pattern of ROS generation in infected cardiac mitochondria as compared to normal controls.

The effect of online addition of specific inhibitors of complex I on the rate of ROS release in glu/mal—energized mitochondria is shown in Fig. 3 and Table 1. The traces of

Table 1 Kinetics of ROS production in glutamate/malate-energized cardiac mitochondria of *T. cruzi*-infected mice±PBN

Incubation with	p moles H_2O_2/min/mg protein		
	Normal	Infected/untreated	Infected/PBN-treated
G/M	3.82±0.89	6.09± 1.51^{a}	4.6±0.23^{b}
G/M→Rot	12.64±1.52^{c}	11.84±2.86^{c}	10.36±1.4^{c}
G/M→Rot→pCMB	1.91±0.31^{c}	1.95±0.43^{c}	ND
G/M→Rot→pCMB→DPI	1.35±0.19^{c}	1.39±0.57^{c}	ND
G/M→pCMB	1.91±0.45^{c}	1.84±0.65^{c}	1.82±0.23^{c}
G/M→DPI	1.54±0.42^{c}	1.49±0.69^{c}	1.54±0.1^{c}
G/M→pCMB→DPI	1.74±0.66^{c}	1.59±0.81^{c}	ND
G/M→Ant	49.7±4.04^{c}	87.48±11.4$^{a,\ c}$	64.64±2.53$^{b,\ c}$
G/M→Myx	19.99±1.47^{c}	31.8±5.53$^{a,\ c}$	21.13±2.9^{b,c}
G/M→Ant→Rot	11.28±2.6^{c}	11.26±2.36^{c}	12.36±1.4^{c}
G/M→Myx→Rot	12.58±1.52^{c}	11.84±0.29^{c}	11.46±0.85^{c}
G/M→Ant→Myx	19.49±1.63^{c}	30.78±4.63$^{a,\ b}$	20.13±2.9$^{b,\ c}$
G/M→Myx→Ant	19.09±4.46^{c}	30.89±4.42$^{a,\ c}$	23.6±3.96$^{b,\ c}$

C3H/HeN mice were infected with *T. cruzi* and treated with phenyl α-butyl-nitrone (PBN). Freshly isolated cardiac mitochondria were energized with complex I substrates (glutamate/malate, G/M), and the rate of H_2O_2 generation was determined with addition of specific inhibitors of the respiratory complexes

Complex I: *Rot* Rotenone, *pCMB* p-chloromercuribenzoate, *DPI* diphenylene iodonium; Complex III: *Ant* Antimycin, *Myx* myxothiazol; ND: not determined

[a] normal-versus-infected/untreated, [b] infected/untreated versus infected/PBN-treated, [c] no treatment versus effect of added inhibitors

$^{a,b,c}p\leq0.01$

Table 2 Kinetics of ROS production in succinate-energized cardiac mitochondria of *T. cruzi*-infected mice±PBN

Incubation with	p moles H_2O_2/min/mg protein		
	Normal	Infected/untreated	Infected/PBN-treated
Succ	2.65±0.36	5.68±0.81[a]	2.02±0.18[b]
Succ→DPI	2.74±0.66	5.59±0.81[a]	ND
Succ→pCMB	2.91±0.58	6.73±0.88[a]	ND
Succ→DPI	2.08±0.34	7.31±1.57[a]	2.89±0.59[b]
Succ→DPI→pCMB	2.54±0.52	8.52±5.07[a]	3.14±0.69[b]
Succ→DPI→pCMB→Rot	2.59±0.39	5.68±0.85[a]	2.12±0.36[b]
Succ→Ant	48.94±6.62[c]	96.12±2.87[a, c]	71.11±15[b, c]
Succ→Myx	26.36±0.46[c]	69.29±2.05[a, c]	24.81±1.64[b, c]
Succ→Ant→Rot	43.27±7.37[c]	89.09±12.02[a, c]	46.71±9.67[b, c]
Succ→Myx→Rot	26.51±0.78[c]	73.08±5.36[a, c]	26.63±2.19[b, c]
Succ→Ant→3-NPA	0.9±0.01[c]	1.94±0.21[c]	0.5±0.06[c]
Succ→Ant→Malo	0.45±0.16[c]	−0.47±1.73[c]	0.55±0.1[c]
Succ→Myx→3-NPA	0.87±0.11[c]	1.64±0.09[c]	0.71±007[c]
Succ→Myx→Malo	0.56±0.25[c]	0.95±0.32[c]	0.83±0.15[c]
Succ→Ant→Myx	24.81±4.78[c]	74.45±8.59[a, c]	19.8±0.55[b, c]
Succ→Ant→Stig	25.74±7.37[c]	69.98±8.80[a, c]	25.38±2.17[b, c]
Succ→Ant→Myx→Rot	26.92±0.47[c]	70.46±2.05[a, c]	17.45±0.55[b, c]
Succ→Ant→Myx→Rot→Stig	25.94±1.27[c]	67.91±1.5[a, c]	20.32±0.83[b, c]
Succ→Myx→Ant	26.2±2.9[c]	67.9±5.52[a, c]	26.31±2.37[b, c]
Succ→Myx→Stig	25.9±1.78[c]	70.84±13.72[a, c]	24.01±4.75[b, c]
Succ→Myx→Rot→Stig	25.12±2.42[c]	71.27±7.15[a, c]	25.82±3.74[b, c]
Succ→Rot→Ant	40.67±8.65[c]	94.93±11.79[a, c]	56.73±4.18[b, c]
Succ→Rot→Ant→Myx	26.87±3.62[c]	71.2±14.43[a, c]	24.67±4.18[b, c]
Succ→Rot→Ant→Stig	25.9±1.78[c]	70.84±13.72[a, c]	24.01±0.48[b, c]
Succ→Rot→Myx	26.54±4.75[c]	69.85±8.31[a, c]	24.4±4.98[b, c]
Succ→Rot→Myx→Ant	26.76±3.01[c]	66.53±6.85[a, c]	25.69±2.07[b, c]
Succ→Rot→Myx→Ant→Stig	26.2±2.9[c]	67.9±5.52[a, c]	26.31±2.3[b, c]

C3H/HeN mice were infected with *T. cruzi* and treated with PBN. Freshly isolated cardiac mitochondria were energized with complex II substrate (succinate, succ), and the rate of H_2O_2 generation was determined with addition of specific inhibitors of the respiratory complexes. Other abbreviations are defined in Table 1

Malo malonate, *3-NPA* 3-nitropropionic acid, *Stig* stigmatellin

amplex red oxidation (Fig. 3a) followed by calculation of the specific rate of ROS release (Fig. 3b) showed that rotenone induced a >2-fold increase in H_2O_2 release in cardiac mitochondria of normal and infected mice. Addition of pCMB (inhibits electron transfer from $[Fe\text{-}S]_{N1a}$ to $[Fe\text{-}S]_{N2}$) or DPI (inhibits electron transfer from FMN to $[Fe\text{-}S]_{N1a}$) (individually or sequentially) completely abolished the rotenone-induced increase in ROS production in all mitochondrial preparations (Fig. 3a,b; Table 1). Addition of pCMB and DPI (without pre-incubation with rotenone) inhibited the glu/mal-dependent H_2O_2 production in all cardiac mitochondrial preparations (Fig. 3c; Table 1). These results show that FMN and the $[Fe\text{-}S]_{N1a}$ center are not the main site of ROS production at the complex I, and electron leakage and $O_2^{\bullet-}$ generation may occur at the sites after $[Fe\text{-}S]_{N1a}$ such as $[Fe\text{-}S]_{N1b}$ or $[Fe\text{-}S]_{N2}$ clusters, or Q_{Nf} ubisemiquinone in murine heart mitochondria (illustrated in Fig. 7). A lack of significant difference in the rate of H_2O_2 production induced by complex I inhibitors in glu/mal-fed cardiac mitochondria from normal and infected mice suggests that complex I is not the site of increased electron leakage and ROS formation in infected murine hearts.

To determine if enhanced ROS production in infected myocardium occurs at complex I during reverse electron flow, we incubated mitochondria with succinate, and determined the effect of complex I inhibitors on the rate of amplex red oxidation. When electrons flow in the reverse direction (from complex II to complex I), addition of DPI (blocks electron transfer from $[Fe\text{-}S]_{N1b}$ cluster to $[Fe\text{-}S]_{N1a}$) or pCMB (blocks electron transfer from $[Fe\text{-}S]_{N2}$ to $[Fe\text{-}S]_{1b}$ cluster) should result in reduced Q site and enhanced electron leakage at $[Fe\text{-}S]_{N1b}$ and Q_{Ns} or Q_{Nf} site (Ohnishi et al. 2005). In our studies, cardiac mitochondria of infected mice exhibited a higher rate of succinate-supported ROS generation than normal controls. Addition of DPI or pCMB (individually or in combination) had no effect on the rate of succinate-supported ROS production in cardiac mitochondria of normal or infected mice (Fig. 4a,b;

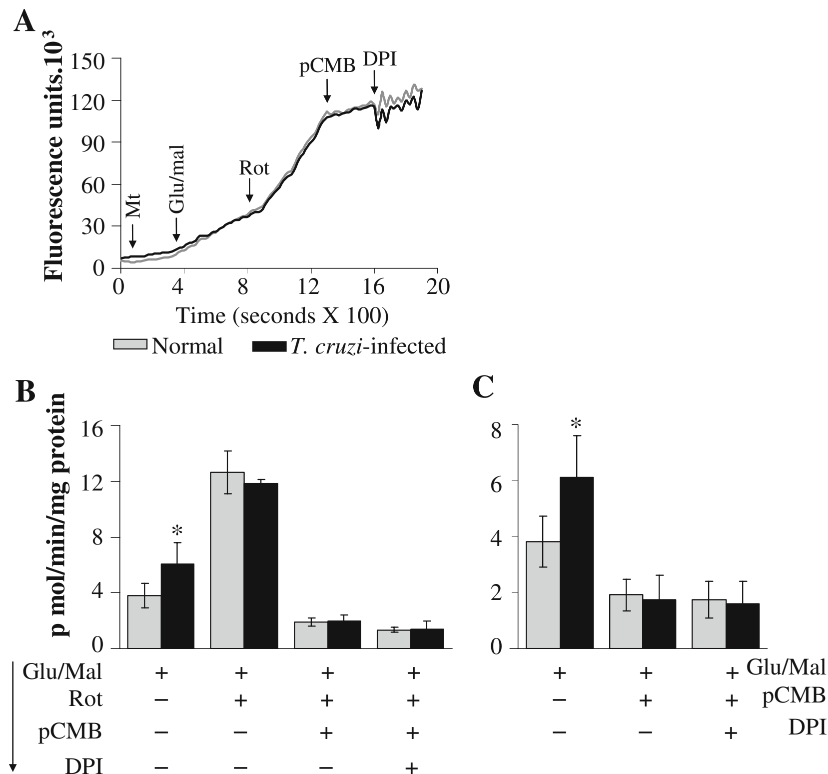

Fig. 3 Complex I is not the site of increased ROS generation in cardiac mitochondria of infected mice. Freshly isolated cardiac mitochondria from normal (*grey*) and infected (*black*) mice were energized with glu/mal, and the rate of H_2O_2 generation was determined in the presence of various inhibitors. **a** Shown are representative traces of kinetics of amplex red oxidation monitored with online addition of complex I inhibitors. **b** & **c** Specific rates of H_2O_2 production in isolated cardiac mitochondria upon online addition of complex I inhibitors (Rot, pCMB, and DPI) were calculated from the kinetic traces. Data (mean±SD) are representative of three independent experiments (n=9/group, $^{*,\#}p<0.01$)

Table 2). These results suggest that succinate-generated electrons flow in the forward direction, maintaining a reduced QH_2/Q pool, and the enhanced ROS formation in cardiac mitochondria of infected mice occurred at a site other than the complex I of the respiratory chain.

Next, we determined whether complex III is the site of increased ROS production in cardiac mitochondria of infected mice using specific inhibitors. The glu/mal-respiring cardiac mitochondria from normal and infected mice exhibited a significant increase in ROS release when treated with antimycin (binds Q_i site near cyt b_H) (Fig. 5a), myxothiazol (binds Q_o site near cyt b_L) (Fig. 5b), or stigmatellin (binds Qo site near ISP protein) (Table 1). The complex III inhibitors-induced ROS release in glu/mal-fed mitochondria was not affected by subsequent addition of complex II inhibitors (malonate or 3-NPA) (data not shown), but was blocked by rotenone addition (Fig. 5a-c; Table 1), thus, validating that mitochondria were indeed respiring complex I substrates. The rate of H_2O_2 production in glu/mal-respiring, antimycin- and myxothiazol-treated cardiac mitochondria of infected mice was 76% and 59% higher than that noted in normal controls, respectively (Fig. 5a,b; Table 1). Subsequent addition of myxothiazol (Fig. 5a; Table 1) after antimycin did not block the higher rate of ROS release in infected mitochondria. The higher rate of ROS production in infected cardiac mitochondria persisted when antimycin was added after myxothiazol (Fig. 5b, d; Table 1). These results suggest that enhanced electron leakage and ROS formation occurs at the Q_o site of the complex III in infected myocardium.

We further validated the role of complex III in increased ROS production in succinate-respiring infected cardiac mitochondria. As above, we noted a substantial increase in the rate of H_2O_2 release in succinate-energized mitochondria of normal and infected mice upon addition of antimycin or myxothiazol (Fig. 6; Table 2). While rotenone had no effect, the antimycin- and myxothiazol-induced ROS generation in succinate-respiring normal cardiac mitochondria was abolished by complex II inhibitors (3-NPA and malonate, Table 2), thus, validating that mitochondria were indeed respiring with succinate as substrate, and maintained forward electron flow. The antimycin-induced increase in ROS generation in succinate-energized normal mitochondria was partially blocked by further

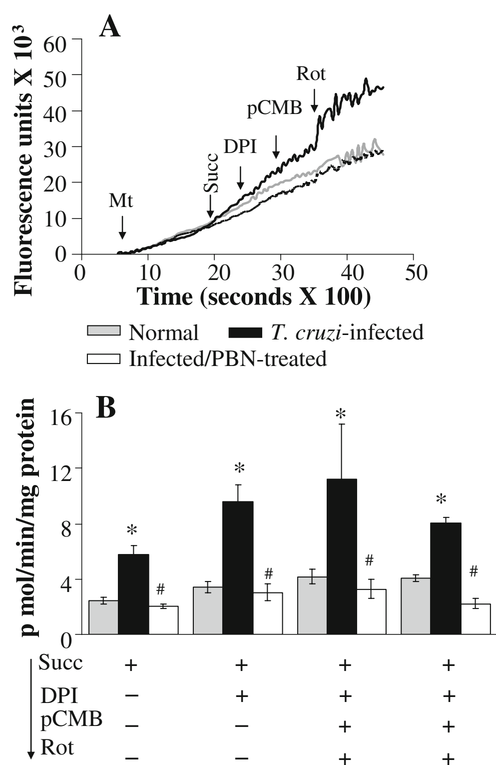

Fig. 4 Reverse flow of electrons from complex II does not contribute to an increased rate of H_2O_2 production in cardiac mitochondria of infected mice. Freshly isolated cardiac mitochondria from normal (*grey*), infected (*black*), and infected/PBN-treated (*white bars* or *broken line*) mice were energized with succinate. **a** Representative traces of amplex red oxidation monitored with online addition of complex I inhibitors (DPI, pCMB, or Rot). **b** The succinate-dependent mitochondrial H_2O_2 production in presence of complex I inhibitors was calculated from the kinetic traces. Data are representative of three independent experiments (n=9/group, $^{*,\#}p<0.01$)

addition of myxothiazol or stigmatellin (individually or in combination) (Fig. 6a; Table 2) as these inhibitors bind to the sites distal to antimycin-binding site, and, thus, restrict electron flow for semiquinone oxidation and $O_2^{\bullet-}$ generation (illustrated in Fig. 7). Antimycin addition did not block the myxothiazol- or stigmatellin-dependent ROS release in succinate-respiring normal mitochondria (Fig. 6b; Table 2), thus, further confirming that ROS release can occur at Q_o site. In succinate respiring cardiac mitochondria of infected mice, antimycin-induced increase in the rate of H_2O_2 production was substantially higher (96%) than the normal controls (Fig. 6a), and the higher rate of ROS release persisted upon subsequent addition of myxothiazol or stigmatellin (Fig. 6a; Table 2). The rate of myxothiazol-induced ROS production in cardiac mitochondria of infected mice was also significantly higher (163% increase) than that observed in normal controls (Fig. 6b, c; Table 2), and persisted upon subsequent addition of antimycin (Fig. 6b) or stigmatellin (Fig. 6c; Table 2). Together, these results confirm that defects at the Q_o site of complex III result in an enhanced electron leakage and ROS production in cardiac mitochondria of infected mice.

The glu/mal- and succinate-energized cardiac mitochondria of PBN-treated/infected mice exhibited a similar response to online addition of complex III inhibitors as was noted in normal controls (Figs. 5, 6; Tables 1, 2). Specifically, the traces of amplex red oxidation showed that online addition of myxothiazol and subsequent inhibitors resulted in a similar rate of ROS release as was noted in glu/mal- (Fig. 5b,d) and succinate- (Fig. 6b,d) fed normal cardiac mitochondria. These data suggest that antioxidant treatment prevented the enhanced leakage of electrons and ROS release through the Q_o site in cardiac mitochondria of infected mice.

Discussion

The present study provides the first direct evidence for the increased ROS production at the complex III site in cardiac mitochondria of mice infected by *T. cruzi*. A decline in the activities of complex I and complex III in chagasic cardiac mitochondria was noted in this and previous (Vyatkina et al. 2004; Wen et al. 2006a) studies. However, the electron transfer impairment leading to an increased leakage of electrons to molecular O_2 and deleterious production of $O_2^{\bullet-}$ in cardiac mitochondria of infected mice occurred primarily due to the defects of complex III. Treatment of infected mice with PBN arrested the increased leakage of electrons and ROS production in cardiac mitochondria that was associated with an improvement in complex III activity and electron transport chain efficiency. Overall, we provide novel data on the mechanisms involved in deleterious ROS production in the myocardium of *T. cruzi*-infected mice.

The defects of complex I have been identified across a wide spectrum of pathologies, including heart failure, and are postulated to contribute to increased ROS production, as well as to deficiency of ATP production (Parker et al. 1990; Gellerich et al. 1999; Genova et al. 2004). The NAD radical (Krishnamoorthy and Hinkle 1988), FMN (Kudin et al. 2004), $[Fe\text{-}S]_{N2}$ (Genova et al. 2001) and $[Fe\text{-}S]_{N1a}$ (Kushnareva et al. 2002) clusters, and complex I-associated ubisemiquinone (Q_{Nf}) (Ohnishi et al. 2005) have been suggested as the site of ROS production in complex I. Our inhibition studies showed that $O_2^{\bullet-}$ release can occur between $[Fe\text{-}S]_{N1}$/$[Fe\text{-}S]_{N2}$ or Q_{Nf}/Q_{Ns} of complex I in murine heart mitochondria (Figs. 3, 7). Despite a decline in complex I activity, we observed no statistically significant difference in the rate of ROS production through complex I in cardiac mitochondria of infected mice (Fig. 3). A slow, but detectable level of reverse flow of electrons (from

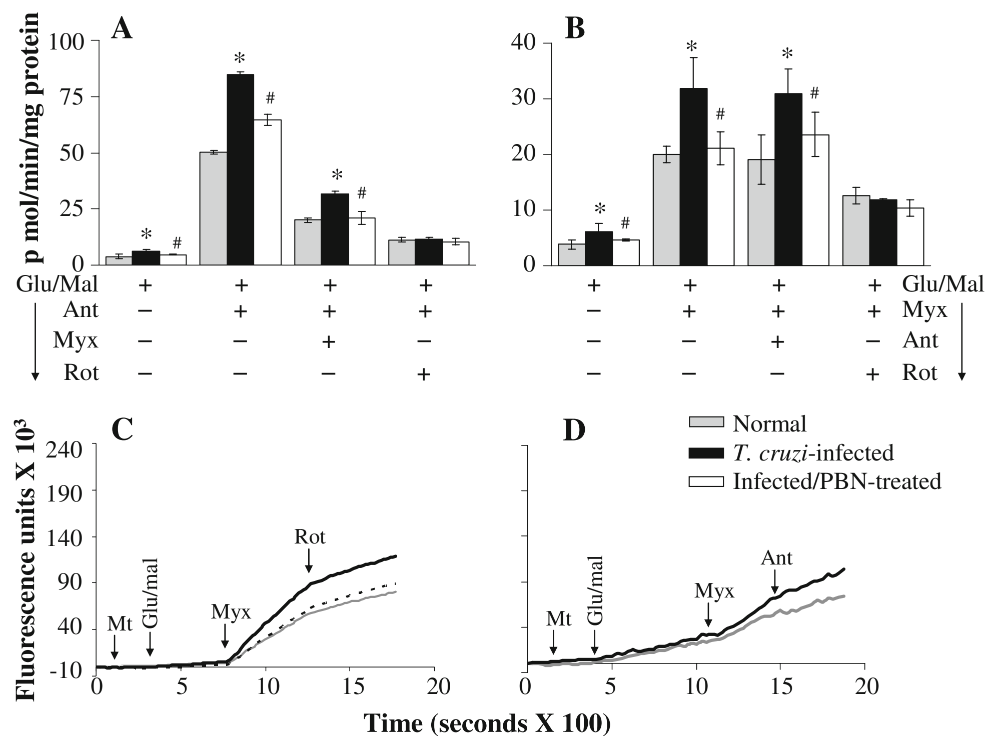

Fig. 5 Kinetics of the rate of H_2O_2 production from complex III in glutamate/malate-energized cardiac mitochondria of infected mice (±PBN). Freshly isolated cardiac mitochondria from normal (*grey*), infected (*black*), and infected/PBN-treated (*white bars* or *broken lines*) mice were energized with glu/mal. **a** & **b** Shown are the effect of online addition of complex III inhibitors (antimycin and myxothiazol) and complex I inhibitor (rotenone) on the rate of H_2O_2 production using amplex red probe. Representative traces are shown in **c** & **d**. Data (mean±SD) are representative of three independent experiments (n=9/group, $^{*,\#}p<0.01$)

complex II-to-complex I) was noted in succinate-oxidizing mitochondria; however, DPI, pCMB, or rotenone did not induce $O_2^{\bullet-}$ production during reverse electron transfer (Fig. 4). Titration of rotenone-induced complex I inhibition showed that >50% loss in complex I activity was required before the rates of electron transport and ATP formation in murine cardiac mitochondria were decreased (unpublished results). We propose that the moderate inhibition of complex I activity (38% decline) in infected mice was below the threshold level to affect the rate of electron transfer and coupling efficiency, and, therefore, complex I was not the site of increased electron leakage and ROS formation in the myocardium of *T. cruzi*-infected mice.

The complex III appeared to be the main site for ROS production in the heart as the antimycin- induced H_2O_2 production rate was stronger compared to that produced by rotenone in glu/mal-fed mitochondria (Tables 1 & 2). According to the Q cycle model of electron transport in complex III, antimycin increases the steady-state concentration of reduced, unstable semiquinone at center Q_o by inhibiting the transfer of electrons through cyt b (Ksenzenko et al. 1983; Turrens et al. 1985; Crofts 2004). Besides antimycin, myxothiazol alone induced a 4-9-fold increase in ROS production in glu/mal- and succinate-fed cardiac mitochondria (Tables 1 & 2). Myxothiazol has been suggested to inhibit complex I (Degli Esposti et al. 1993). In our study, myxothiazol-induced H_2O_2 generation in glu/mal-energized mitochondria was rotenone-sensitive (Fig. 5b); however, rotenone had no effect on myxothiazol-induced H_2O_2 release when succinate was used as a substrate (Fig. 6c; Table 2). These data show that complex I is not the site of myxothiazol-induced ROS production in murine cardiac mitochondria. The finding that antimycin did not suppress the myxothiazol-induced H_2O_2 production (Fig. 5b,d; Table 1) suggests that myxothiazol stimulates ROS production at a site proximal to that of the antimycin-inhibiting site in the electron flow (Fig. 7). Our data are supported by others documenting the myxothiazol-induced ROS production in rat hearts and brain mitochondria (Starkov and Fiskum 2001; Gyulkhandanyan and Pennefather 2004) and in liver hepatocyte mitochondria (Young et al. 2002).

Several observations support the notion that defects in the complex III led to an increased mitochondrial ROS production in *T. cruzi*-infected myocardium. Disease pathology in cardiac failure during ischemia/reperfusion (Towbin et al. 1999) and the effects of neurological and age-related diseases, e.g., Alzheimer's (Aleardi et al. 2005), Parkinson's and Huntington (Schapira 1999), have been attributed to a loss in respiratory complex activities. We have shown that the specific activity of complex III is compromised during *T. cruzi* infection and cardiac disease development (Vyatkina et al. 2004; Wen et al. 2006a). As little as a 15% inhibition of complex III can lead to a defect in electron transfer function for ATP synthesis in murine cardiac mitochondria (unpublished observations). Inhibition studies showed that a deficiency in complex III activity is manifested as leakage of electrons through the Q_o site and increased $O_2^{\bullet-}$ formation in cardiac mitochondria of infected mice (Fig. 5, 6; Tables 1, 2).

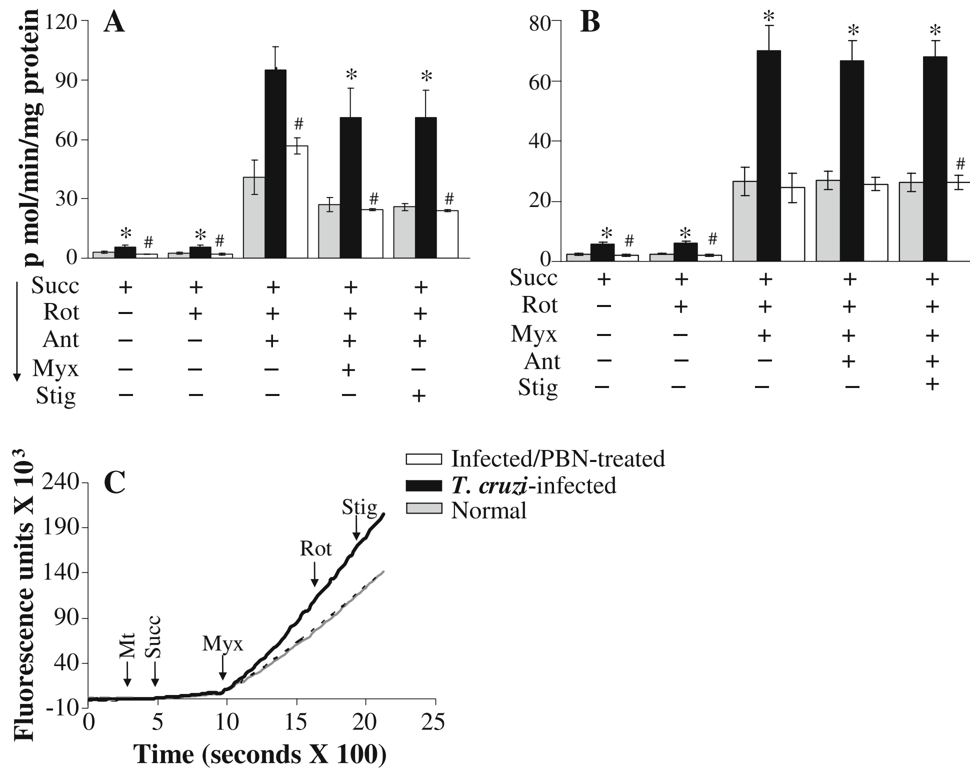

Fig. 6 Kinetics of the rate of H_2O_2 production from complex III in succinate-energized cardiac mitochondria of infected mice (±PBN). Freshly isolated cardiac mitochondria from normal (*grey*), infected (*black*), and infected/PBN-treated (*white bar* or *broken line*) mice were energized with succinate. **a** & **b** Specific rates of mitochondrial H_2O_2 production were calculated from the kinetic traces of amplex red oxidation with online addition of complex I (rotenone) and complex III (antimycin, myxathiazol or stigmatellin) inhibitors. Representative traces are shown in panel **c**. Data are representative of three independent experiments (n=9/group, $^{*,\#}p$<0.01)

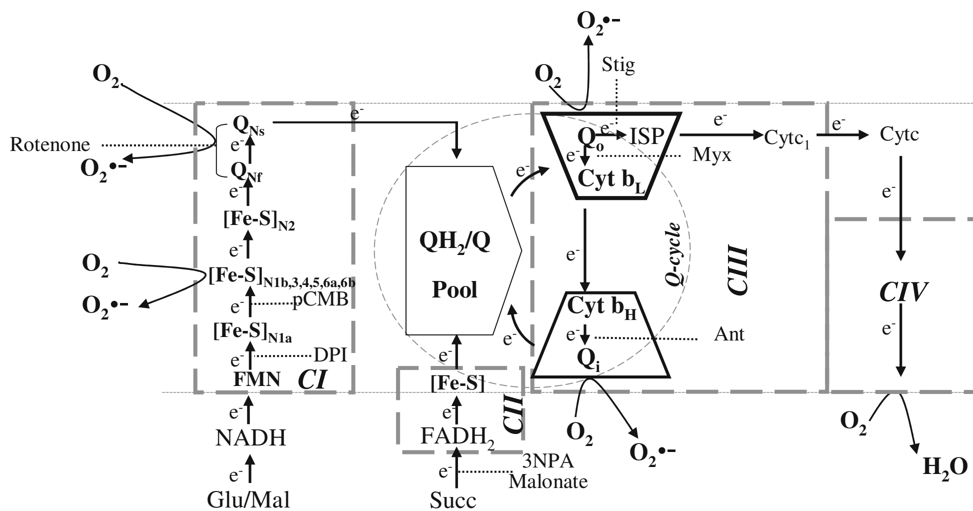

Fig. 7 Schematic representation of electron transport chain to illustrate the site of increased $O_2^{\bullet-}$ release in cardiac mitochondria of infected mice. Electrons enter complex III via the QH_2/Q pool from complex I or complex II. Quinol is oxidized in a bifurcated manner with electron transfer to cyt b_L and ISP. Electrons at cyt b equilibrate between cyt b_L and cyt b_H. The sites of inhibition of complex I by Rot, pCMB and DPI, complex II by 3-NPA and malonate, and of complex III by Ant, Myx, and Stig are shown. *Dotted arrows* show the putative inhibition of electron flow at the complex I and complex III. The *curved black arrows* mark the site(s) of $O_2^{\bullet-}$ production in mitochondria

The three-dimensional structure of complex III and our data provide insights into the nature of the complex III defects in infected myocardium. First, cyt c1, along with ISP protein and cyt b, forms the inter-membrane associated central catalytic domain of complex III (Robertson et al. 1993). We have shown that complex III contain oxidatively modified core proteins (Wen and Garg 2004) that, with a high sequence similarity to soluble, matrix-processing peptidases (MPP) (Braun and Schmitz 1995), are thought to be involved in the cleavage and processing of the signal sequence of the ISP protein (Iwata et al. 1998). The oxidatively modified core proteins may not process the pre-sequence of ISP. Incorporation of the mis-folded ISP in complex III may result in mis-assembly of the catalytic site and inhibition of the complex III activity.

Secondly, myxothiazol and stigmatellin bind to different domains within the Q_o site. Stigmatellin binds to the distal domain of Q_o towards ISP, while myxothiazol binds to the proximal domain (near cyt b_L). In cardiac mitochondria of infected mice, the increased electron leakage at the Q_o site was observed with myxothiazol. In forward electron transfer, stigmatellin did not inhibit electron flow through the myxothiazol site, and, thus, did not eliminate the response to myxothiazol. These data suggest the defects of the Q_o site are accrued toward the cyt b_L in infected myocardium. In *Rhodobacter*, five point mutations at cyt b elicited resistance to myxothiazol, one of which (Y132) also affected the complex III activity (Crofts 2004). In other studies, we have noted that cyt b expression is decreased in chagasic myocardium and results in assembly of cyt b-depleted complex III that is not enzymatically active (unpublished observations). These observations allow us to propose that incorporation of cyt b that is oxidized at the Y132 site and/or assembly of cyt b-depleted complex III result in enhanced electron leakage and $O_2^{\bullet-}$ production in chagasic cardiac mitochondria.

PBN-dependent normalization of ROS production in cardiac mitochondria of infected mice was an outcome of several factors. One, PBN is an efficient scavenger of ROS (Floyd et al. 2002). Second, PBN-mediated decreased oxidation of mitochondrial membranes improved the mitochondrial efficiency of electron transport and oxidative phosphorylation (Wen et al. 2006a). Third, PBN-dependent preservation of the complex III activity, control of glu/mal- and succinate-dependent ROS production at the complex III site, and normalization of the myxothiazol-resistant increase in $O_2^{\bullet-}$ production in chagasic cardiac mitochondria suggests that PBN treatment prevented the oxidation-induced modification of the Q_o site.

In summary, the present study shows that cardiac mitochondria of *T. cruzi*-infected mice sustain increased ROS production due to defects at the Q_o site (towards cyt b_L) that result in increased electron leakage to molecular oxygen and ROS production. The potential role of oxidation-induced modification of the Q_o site that can result in decreased complex III activity as well as increased electron leakage is evidenced by the inhibition of loss in complex III activity and ROS formation in infected mice treated with PBN.

Acknowledgements This work was supported by a grant (AI054578) from the National Institute of Allergy and Infectious Diseases/National Institutes of Health to NJG. Our thanks are due to Ms. Mardelle Susman for editing the manuscript.

References

Aleardi AM, Benard G et al (2005) "Gradual alteration of mitochondrial structure and function by beta-amyloids: importance of membrane viscosity changes, energy deprivation, reactive oxygen species production, and cytochrome c release". J Bioenerg Biomembr 37(4):207–25

Boveris A, Oshino N et al (1972) "The cellular production of hydrogen peroxide". Biochem J 128(3):617–30

Bradford MM (1976) "A rapid and sensitive method for the quantitation of microgram quantities of protein utilizing the principle of protein-dye binding". Anal Biochem 72:248–54

Braun HP, Schmitz UK (1995) "Are the 'core' proteins of the mitochondrial bc1 complex evolutionary relics of a processing protease?". Trends Biochem Sci 20(5):171–5

Carrasco Guerra HA, Palacios-Pru E et al (1987) "Clinical, histochemical, and ultrastructural correlation in septal endomyocardial biopsies from chronic chagasic patients: detection of early myocardial damage". Am Heart J 113(3):716–24

Crofts AR (2004) "The cytochrome bc1 complex: function in the context of structure". Annu Rev Physiol 66:689–733

Degli Esposti M, Ghelli A et al (1993) "Complex I and complex III of mitochondria have common inhibitors acting as ubiquinone antagonists". Biochem Biophys Res Commun 190(3):1090–6

Floyd RA, Hensley K et al (2002) "Nitrones as neuroprotectants and antiaging drugs". Ann N Y Acad Sci 959:321–9

Garg N, Popov VL et al (2003) "Profiling gene transcription reveals a deficiency of mitochondrial oxidative phosphorylation in *Trypanosoma cruzi*-infected murine hearts: implications in chagasic myocarditis development". Biochim Biophys Acta 1638(2):106–20

Gellerich FN, Trumbeckaite S et al (1999) "Impaired energy metabolism in hearts of septic baboons: diminished activities of Complex I and Complex II of the mitochondrial respiratory chain". Shock 11(5):336–41

Genova ML, Pich MM et al (2004) "The mitochondrial production of reactive oxygen species in relation to aging and pathology". Ann N Y Acad Sci 1011:86–100

Genova ML, Ventura B et al (2001) "The site of production of superoxide radical in mitochondrial Complex I is not a bound ubisemiquinone but presumably iron-sulfur cluster N2". FEBS Lett 505(3):364–8

Gyulkhandanyan AV, Pennefather PS (2004) "Shift in the localization of sites of hydrogen peroxide production in brain mitochondria by mitochondrial stress". J Neurochem 90(2):405–21

Harper A (1963) "Glucose-6-Phosphatase". Methods of enzymatic analysis:788–792

Iwata S, Lee JW et al (1998) "Complete structure of the 11-subunit bovine mitochondrial cytochrome bc1 complex". Science 281 (5373):64–71

Jarreta D, Orus J et al (2000) “Mitochondrial function in heart muscle from patients with idiopathic dilated cardiomyopathy”. Cardiovasc Res 45(4):860–5

Krishnamoorthy G, Hinkle PC (1988) “Studies on the electron transfer pathway, topography of iron-sulfur centers, and site of coupling in NADH-Q oxidoreductase”. J Biol Chem 263(33):17566–75

Ksenzenko M, Konstantinov AA et al (1983) “Effect of electron transfer inhibitors on superoxide generation in the cytochrome bc1 site of the mitochondrial respiratory chain”. FEBS Lett 155 (1):19–24

Kudin AP, Bimpong-Buta NY et al (2004) “Characterization of superoxide-producing sites in isolated brain mitochondria”. J Biol Chem 279(6):4127–35

Kushnareva Y, Murphy AN et al (2002) “Complex I-mediated reactive oxygen species generation: modulation by cytochrome c and NAD(P)+ oxidation-reduction state”. Biochem J 368(Pt 2):545–53

Lemasters JJ (1984) “The ATP-to-oxygen stoichiometries of oxidative phosphorylation by rat liver mitochondria. An analysis of ADP-induced oxygen jumps by linear nonequilibrium thermodynamics”. J Biol Chem 259(21):13123–30

Lui NS, Roels OA et al (1968) “Subcellular distribution of enzymes in Ochromonas malhamensis”. J Protozool 15(3):536–42

Ohnishi ST, Ohnishi T et al (2005) “A possible site of superoxide generation in the complex I segment of rat heart mitochondria”. J Bioenerg Biomembr 37(1):1–15

Palacios-Pru E, Carrasco H et al (1989) “Ultrastructural characteristics of different stages of human chagasic myocarditis”. Am J Trop Med Hyg 41(1):29–40

Parker WD Jr, Boyson SJ et al (1990) “Evidence for a defect in NADH: ubiquinone oxidoreductase (complex I) in Huntington’s disease”. Neurology 40(8):1231–4

Robertson DE, Ding H et al (1993) “Hydroubiquinone-cytochrome c2 oxidoreductase from Rhodobacter capsulatus: definition of a minimal, functional isolated preparation”. Biochemistry 32 (5):1310–7

Sanz A, Caro P et al (2005) “Dietary restriction at old age lowers mitochondrial oxygen radical production and leak at complex I and oxidative DNA damage in rat brain”. J Bioenerg Biomembr 37(2):83–90

Schapira AH (1999) “Mitochondrial involvement in Parkinson’s disease, Huntington’s disease, hereditary spastic paraplegia and Friedreich’s ataxia”. Biochim Biophys Acta 1410(2):159–70

Starkov AA, Fiskum G (2001) “Myxothiazol induces H(2)O(2) production from mitochondrial respiratory chain”. Biochem Biophys Res Commun 281(3):645–50

Toth PP, Ferguson-Miller SM et al (1986) “Isolation of highly coupled heart mitochondria in high yield using a bacterial collagenase”. Methods Enzymol 125:16–27

Towbin JA, Bowles KR et al (1999) “Etiologies of cardiomyopathy and heart failure”. Nat Med 5(3):266–7

Turrens JF, Alexandre A et al (1985) “Ubisemiquinone is the electron donor for superoxide formation by complex III of heart mitochondria”. Arch Biochem Biophys 237(2):408–14

Vyatkina G, Bhatia V et al (2004) “Impaired mitochondrial respiratory chain and bioenergetics during chagasic cardiomyopathy development”. Biochim Biophys Acta 1689:162–173

Wen J-J, Bhatia V et al (2006a) “Phenyl-alpha-tert-butyl nitrone reverses mitochondrial decay in acute Chagas disease”. Am J Pathol 169(6):1953–64

Wen J-J, Garg N (2004) “Oxidative modifications of mitochondrial respiratory complexes in response to the stress of Trypanosoma cruzi infection”. Free Radic Biol Med 37(12):2072–81

Wen J-J, Vyatkina G et al (2004) “Oxidative damage during chagasic cardiomyopathy development: Role of mitochondrial oxidant release and inefficient antioxidant defense”. Free Radic Biol Med 37(11):1821–33

Wen J-J, Yachelini PC et al (2006b) “Increased oxidative stress is correlated with mitochondrial dysfunction in chagasic patients”. Free Rad Biol Med 41:270–276

World Health Organization (2002) Control of Chagas disease: Second report of the WHO expert committee. WHO Technical Report Series 905. UNDP/World Bank/WHO, Geneva, Switzerland

Young TA, Cunningham CC et al (2002) “Reactive oxygen species production by the mitochondrial respiratory chain in isolated rat hepatocytes and liver mitochondria: studies using myxothiazol”. Arch Biochem Biophys 405(1):65–72

Zacks MA, Wen J-J et al (2005) “An overview of chagasic cardiomyopathy: pathogenic importance of oxidative stress”. Ann Acad Bras Cienc 77:695–715